




Modified substrate specificity of a methyltransferase domain by protein insertion into an adenylation domain of the bassianolide synthetase

Fuchao Xu¹, Russell Butler², Kyle May², Megi Rexhepaj², Dayu Yu^{1,3}, Jiachen Zi¹, Yi Chen¹, Yonghong Liang^{1,4}, Jia Zeng¹, Joan Hevel^{2*} and Jixun Zhan^{1*} 

Abstract

Background: Creating designer molecules using a combination of select domains from polyketide synthases and/or nonribosomal peptide synthetases (NRPS) continues to be a synthetic goal. However, an incomplete understanding of how protein-protein interactions and dynamics affect each of the domain functions stands as a major obstacle in the field. Of particular interest is understanding the basis for a class of methyltransferase domains (MT) that are found embedded within the adenylation domain (A) of fungal NRPS systems instead of in an end-to-end architecture.

Results: The MT domain from bassianolide synthetase (BSLS) was removed and the truncated enzyme BSLS- Δ MT was recombinantly expressed. The biosynthesis of bassianolide was abolished and *N*-desmethylbassianolide was produced in low yields. Co-expression of BSLS- Δ MT with standalone MT did not recover bassianolide biosynthesis. In order to address the functional implications of the protein insertion, we characterized the *N*-methyltransferase activity of the MT domain as both the isolated domain (MT_{BSLS}) and as part of the full NRPS megaenzyme. Surprisingly, the MT_{BSLS} construct demonstrated a relaxed substrate specificity and preferentially methylated an amino acid (L-Phe-SNAC) that is rarely incorporated into the final product. By testing the preference of a series of MT constructs (BSLS, MT_{BSLS}, cMT, XLcMT, and aMT) to L-Phe-SNAC and L-Leu-SNAC, we further showed that restricting and/or fixing the termini of the MT_{BSLS} by crosslinking or embedding the MT within an A domain narrowed the substrate specificity of the methyltransferase toward L-Leu-SNAC, the preferred substrate for the BSLS megaenzyme.

Conclusions: The embedding of MT into the A2 domain of BSLS is not required for the product assembly, but is critical for the overall yields of the final products. The substrate specificity of MT is significantly affected by the protein context within which it is present. While A domains are known to be responsible for selecting and activating the biosynthetic precursors for NRPS systems, our results suggest that embedding the MT acts as a secondary gatekeeper for the assembly line. This work thus provides new insights into the embedded MT domain in NRPSs, which will facilitate further engineering of this type of biosynthetic machinery to create structural diversity in natural products.

Keywords: Nonribosomal peptide synthetase, Methyltransferase domain, Substrate specificity, Domain removal, Heterologous expression, In vitro reaction

* Correspondence: joanie.hevel@usu.edu; jixun.zhan@usu.edu

²Department of Chemistry and Biochemistry, Utah State University, 0300 Old Main Hill, Logan, UT 84322-0300, USA

¹Department of Biological Engineering, Utah State University, 4105 Old Main Hill, Logan, UT 84322-4105, USA

Full list of author information is available at the end of the article



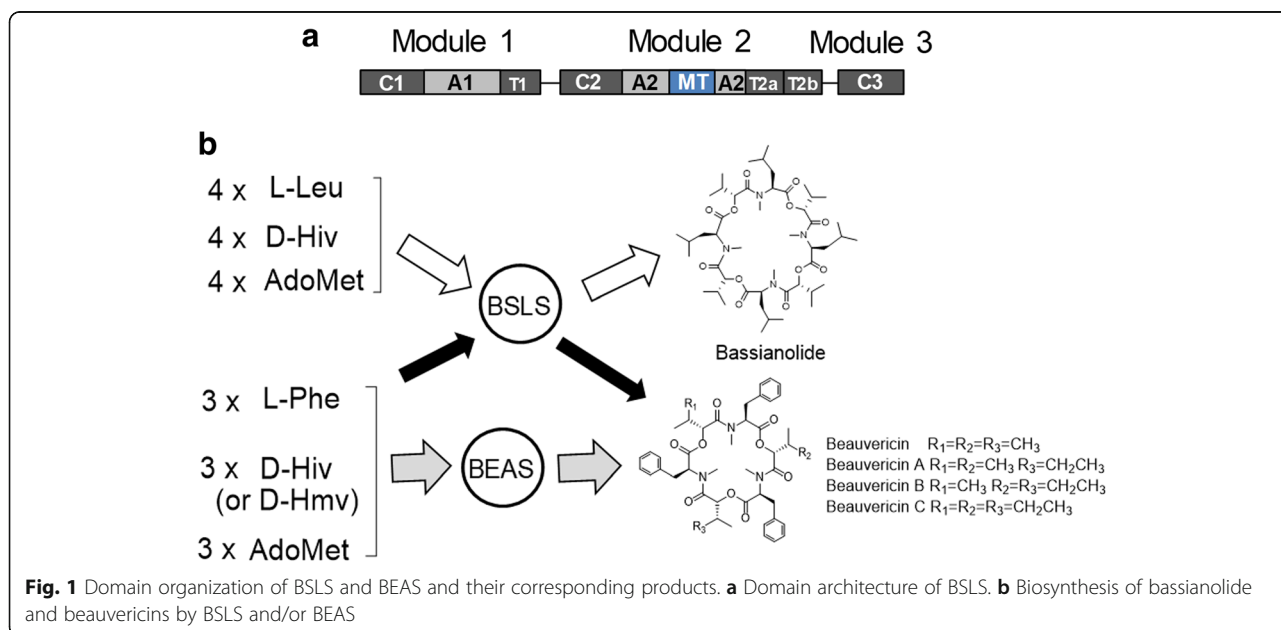
Introduction

Modular enzymes are widely involved in the biosynthesis of many biologically important molecules including both primary (fatty acids) and secondary metabolites (natural products). Natural product megasynthetases, which include polyketide synthases (PKSs), nonribosomal synthetases (NRPSs), and hybrid forms, typically combine a series of catalytic domains – often as a single polypeptide – to assemble simple molecules into a variety of structurally and functionally diverse molecules [1]. NRPSs contain three essential core domains for chain elongation, including adenylation (A), thiolation (T or PCP) and condensation (C) domains, which are combined end-on-end to form independent modules. The precursor molecule for each module is selected by an A domain, and activated for transfer to a T domain. Thus, A domains are thought to function as the primary gate keepers for precursor selection. C domains condense two units of activated precursors to form the corresponding amide or ether bonds for downstream chain elongation. Additional tailoring domains may also be present, such as epimerization (E), thioesterase (TE), and methyltransferase (MT) domains, each of which contributes to the chemical diversity and bioactivity of natural products [2]. Coordinated communication between each of these catalytic domains is essential, but the molecular mechanisms underlying this process are poorly understood.

A unique feature of MT-containing NRPSs is that the MT domains are embedded within the A domains rather than being located adjacent to independent domains [3]. The rationale for this placement in NRPSs is unknown but suggests that the MT may undergo significant

motions during natural product synthesis. A recent structure of an embedded NRPS MT supports this hypothesis [4]. Furthermore, the general observation that protein domain insertions are often associated with a gain-in-function of switch-like behavior [5, 6] makes for the intriguing possibility that the MT takes on a much larger role in natural product synthesis than simple methyl transfer. Embedding the MT into the A domain may act as scaffolding or may modulate substrate specificity, activity and interdomain communication.

One such embedded MT exists in BSLs, the fungal NRPS that synthesizes the cyclic octadepsipeptide bassianolide. The modular BSLs enzyme (C1-A1-T1-C2-A2-MT-A2-T2a-T2b-C3, Fig. 1) can be found in several fungi such as *Beauveria bassiana* [7]. *B. bassiana* also produces a cyclic hexadepsipeptide, beauvericin, and the corresponding beauvericin synthetase (BEAS) has the same domain organization (Fig. 1a) [8]. Bassianolide and beauvericin have shown anticancer activities and are synthesized from amino acid and hydroxyl acid precursors [9, 10]. We have previously investigated the three C domains and the twin T2 domains in these NRPSs, and revealed that this type of NRPS uses an “alternative incorporation” approach to extend the depsipeptide chain and C3 plays a role of decision maker in the chain length control [11]. Interestingly, BSLs is flexible with both the amino acid and hydroxyl acid precursors; i.e., it produces bassianolide as the major product (containing *N*-methyl-L-Leu), together with small amounts of beauvericin and its analogs beauvericins A-C (containing *N*-methyl-L-Phe) (Fig. 1b). By contrast, BEAS is strict with the amino acid precursor and only has some flexibility with hydroxyl acid



units, D-2-hydroxyisovalerate (D-Hiv) and D-2-hydroxy-3-methylvalerate (D-Hmv), to yield beauvericins (Fig. 1b). This finding suggests that the MT, as well as other catalytic domains in BSLS, have relatively relaxed substrate specificities. Therefore, BSLS was selected in this work to understand the role of the embedded MT and how its substrate specificity may be affected by the protein insertion. Our results demonstrate that the presence of a MT domain in BSLS is not essential for the product assembly, but is critical for the overall yields of the final products. Moreover, embedding the MT in the BSLS NRPS is used to tune the substrate specificity of the MT and thus functions as a secondary substrate gate keeper. This work thus provides new insights into the embedded MT domain in NRPSs, which will facilitate further engineering of this type of biosynthetic machinery to create structural diversity in natural products.

Results

A functional MT domain is not essential for NRP assembly

To examine the structural necessity of the MT domain within BSLS, we constructed BSLS- Δ MT through splicing by overlap extension (SOE) PCR and tested whether nonribosomal peptide (NRP) products can still be synthesized without the *N*-MT domain. Both BSLS and BEAS were functionally expressed in *Saccharomyces cerevisiae* BJ5464-NpgA in our previous work to yield their corresponding products [12]. Therefore, this strain was used to express BSLS- Δ MT for product analysis. LC-MS analysis revealed that the engineered enzyme BSLS- Δ MT yielded no bassianolide, but a more polar product (Fig. 2a). ESI-MS of this new product showed several ion peaks, including $[M + H]^+$ at m/z 853.4, $[M + NH_4]^+$ at m/z 870.5, $[M + Na]^+$ at m/z 875.4, and $[M + K]^+$ at m/z 891.4 (Additional file 1: Figure S1), indicating that this product has a molecular weight of 852. This is 56 mass units (equivalent to four CH_2 groups) less than bassianolide, suggesting that this compound is *N*-desmethylbassianolide (Fig. 2a).

Due to the low yield of this nonmethylated product, we did not purify it for NMR analysis. Considering the yield of beauvericin and its analogs (beauvericins A-C) produced by BEAS in yeast is much higher than bassianolide, we rationalized that it might be easier to generate sufficient amounts of demethylated derivative of beauvericin. We also wanted to distinguish if the low product yields were a result of the absence of the MT domain or the absence of MT activity. To this end, we used a different approach to examine the MT domain in BEAS. Based on the alignment of BEAS with other reported MTs, it was found that the MT domain of BEAS contains a $G_{2129}TG_{2133}$ motif, which is consistent with the consensus $GxGxG$ sequence that is a part of the *S*-adenosyl methionine (AdoMet) binding site [13].

Therefore, we mutated the middle G residue at position 2131 to interrupt the binding of AdoMet. We constructed BEAS-G2131A (pDY170) in a yeast expression vector and expressed it in *S. cerevisiae* BJ5464-NpgA. As shown in Fig. 2b, three new products, but not beauvericins, were formed by this mutant. Their molecular weights were determined to be 741, 755 and 768, respectively, based on the ESI-MS spectra (Additional file 1: Figure S1), corresponding to the demethylated derivatives of beauvericin, beauvericin A and beauvericin B. The major product at 7.1 min was isolated for NMR analysis, which confirmed that this product is *N*-desmethylbeauvericin (Additional file 1: Figures S2-S4) and that G2131 is a critical AdoMet binding site residue. We next constructed a yeast expression plasmid (pFC31) that only harbors the MT domain of BSLS. Co-expression of the isolated MT_{BSLS} with BSLS- Δ MT to induce *trans* methylation yielded only the demethylated product (Additional file 1: Figure S5A). Similarly, co-expression of MT_{BEAS} (pDY268) with BEAS-G2131A in the yeast did not recover the biosynthesis of beauvericins (Additional file 1: Figure S5B), suggesting that natural embedding of a functional MT domain in A2 is required to form the methylated NRPs.

Heterologous expression and functional characterization of the MT domain from BSLS

In order to determine whether embedding the MT domain into the A2 domain affects MT activity, we sought to compare the methyltransferase activity of the isolated MT domain (MT_{BSLS}) to the methyltransferase activity of the full megaenzyme (BSLS). The gene fragment encoding the MT domain in BSLS was cloned from the genomic DNA of *B. bassiana* into a pET28a expression vector. The MT domain was expressed in *E. coli* BL21-CodonPlus (DE3)-RIL strain (hereafter referred to as RIL) cells as a His₆-tagged protein and was purified using Ni-NTA resin. The methyltransferase activity of the isolated MT domain (MT_{BSLS}) was directly assessed using the synthetic substrate mimic aminoacyl-*N*-acetylcysteamine thioesters (aminoacyl-SNACs) to avoid the need for the A or T domains [14]. Because bassianolide contains *N*-methyl-L-Leu, L-Leu-T2a (or -T2b) is believed to be the natural substrates. Thus, we synthesized L-Leu-SNAC as a mimicking substrate. HPLC analysis showed that incubation of MT_{BSLS} with AdoMet and L-Leu-SNAC led to the formation of a new peak in the chromatogram (Fig. 3a). ESI-MS spectrum (Fig. 3b) indicated that this product has a molecular weight of 246, which is 14 mass units more than the substrate and consistent with *N*-methyl-L-Leu-SNAC. These results show that the isolated MT domain from BSLS is active with its cognate substrate. In our previous study [15], we

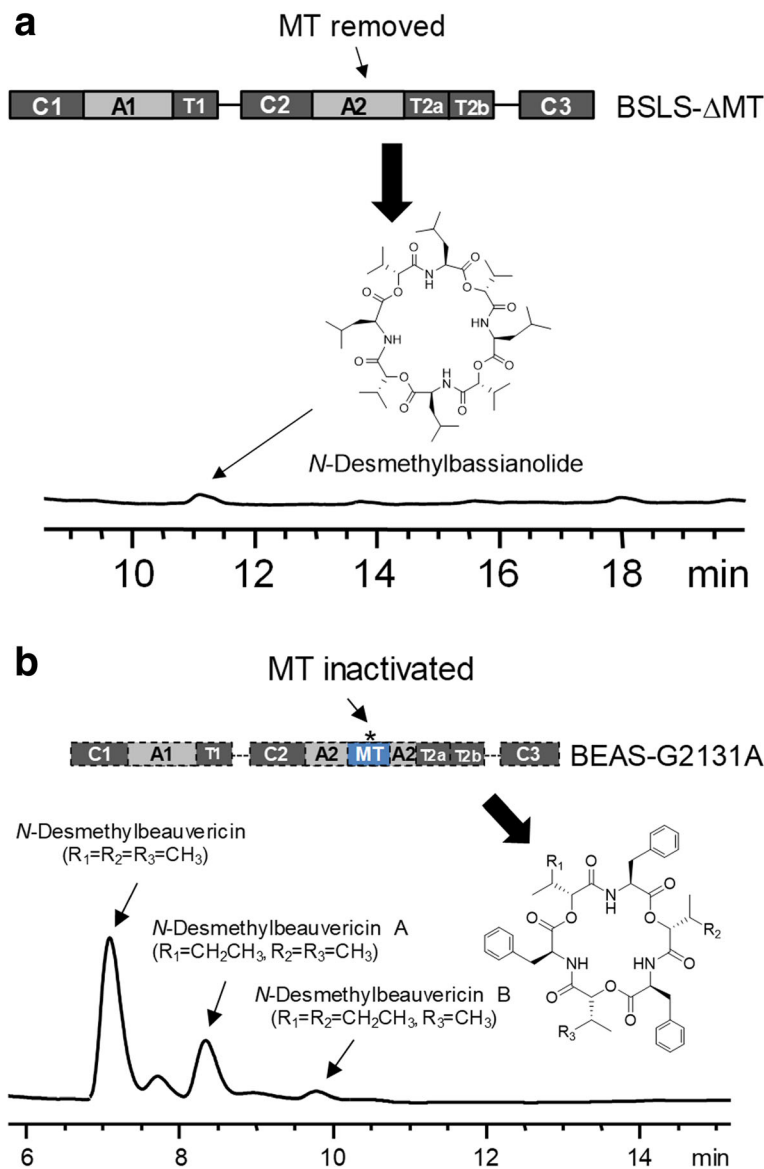


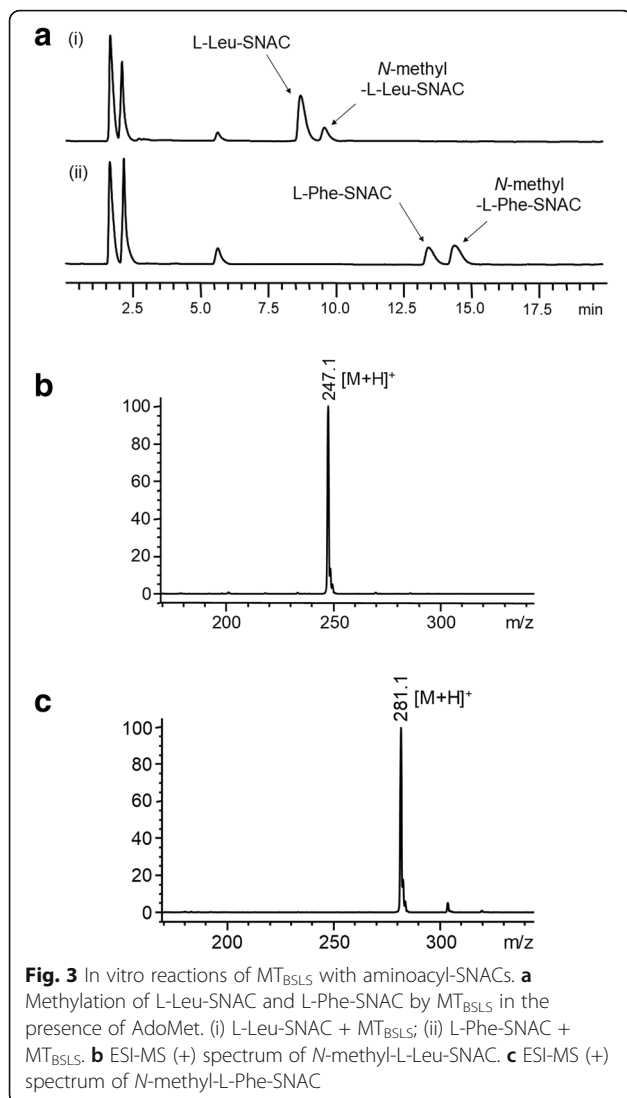
Fig. 2 Biosynthesis of *N*-desmethylbassianolide (a) by BSLs- Δ MT (MT removed) and *N*-desmethylbeauvericins (b) by BEAS-G2131A (MT inactivated)

found that BSLs can also synthesize beauvericin and its analogs beauvericins A-C when it was expressed in *S. cerevisiae* BJ5464-NpgA, suggesting that MT_{BSLs} can also methylate L-Phe-SNAC. Reaction of MT_{BSLs} with L-Phe-SNAC indeed gave rise to *N*-methyl-L-Phe-SNAC (trace ii, Fig. 3a), which was confirmed by its ESI-MS spectrum (Fig. 3c).

Substrate specificity of the isolated MT domain of BSLs

Given the apparent flexibility of MT_{BSLs} to use both L-Phe-SNAC and L-Leu-SNAC as substrates, we sought to determine how broad the substrate specificity of MT_{BSLs} is. Therefore, we synthesized two additional aminoacyl-SNACs, L-Ile-SNAC and L-Val-SNAC, for in vitro assays of MT_{BSLs}.

However, only a tiny portion of substrates were converted into *N*-methylated products, which were detected by ESI-MS analysis (Additional file 1: Figure S6A and B). In order to determine whether MT_{BSLs} displayed a preference for L-Leu-SNAC or L-Phe-SNAC, we measured the rate of methylation of these two substrates as a function of substrate concentration. The methylation assay utilized radiolabeled AdoMet (³H-AdoMet) as the methyl group donor in order to quantify the levels of methyl groups transferred (Fig. 4a). Interestingly, even though BSLs predominantly synthesizes bassianolide that contains the *N*-methyl-L-Leu moiety [12, 15], the isolated MT_{BSLs} enzyme was observed to possess a much higher rate of methylation with L-Phe-SNAC (V_{max} of $0.41 \pm 0.040 \mu\text{M}/\text{min}$) than with L-Leu-



SNAC (V_{max} of $0.05 \pm 0.01 \mu\text{M}/\text{min}$) and a smaller K_m ($0.46 \pm 0.17 \mu\text{M}$ for Phe-SNAC and $2.8 \pm 1.3 \mu\text{M}$ for Leu-SNAC) (Fig. 4b).

The substrate specificity of MT_{BSLs} is affected by protein context

Intrigued by the observation that the BSLs system produces more NRP with *N*-methyl-L-Leu, but the isolated MT_{BSLs} prefers to methylate L-Phe-SNAC, we tested the ability of the intact MT in BSLs to methylate both L-Phe-SNAC and L-Leu-SNAC at a fixed substrate concentration. Compared to the isolated MT_{BSLs} that methylated Phe-SNAC > 7-fold more than L-Leu-SNAC, the embedded MT in BSLs methylated both amino acid derivatives similarly (Fig. 5). In order to gain more structural insight regarding the potential structural differences that might occur between embedded and isolated MT_{BSLs} , we used the recent crystal structure of an

embedded MT domain from the TioS NRPS cluster to create a homology model for MT_{BSLs} (Fig. 6a) [16–20]. The TioS structure includes both the MT (with the product *S*-adenosylhomocysteine bound) and A domains which allowed us to examine the predicted MT active site and how the two domains are connected.

The MT in $TioS(A_{4a}M_4A_{4b})$ *N*-methylates L-Val and norcoronamic acid (NCA), and to a lesser extent L-Ile [4]. On the other hand, MT_{BSLs} preferentially *N*-methylates L-Phe and to a lesser extent L-Leu. Although all five substrates in question are all hydrophobic, we found it surprising that all the residues in MT_{4TioS} that are predicted to interact with the side chain of the amino acid substrate are identical between MT_{4TioS} and MT_{BSLs} (Additional file 1: Fig. 6b, c and Additional file 1: Figure S7). This suggests that characteristics other than side chain identities help to govern substrate specificity of the methyltransferase.

In evaluating the $TioS(A_{4a}M_4A_{4b})$ structure, we noted that the backbone of the N-terminal and C-terminal residues of the MT domain reside within $\sim 6 \text{ \AA}$ of each other, and that the positioning of the termini may be governed by the connection to the A domain. Given that the N-terminus of the MT resides at the end of the helix that acts as the bottom of the methyltransferase active site, we rationalized that altering the distance, conformation, or flexibility between the termini (e.g., in the isolated MT_{BSLs}) may affect methyltransferase activity.

In order to test the theory that increased flexibility or conformation in the N- and C-termini of the isolated MT_{BSLs} affected substrate preference, we designed and purified a construct of MT_{BSLs} that contained an additional cysteine residue at both ends (cMT). We then crosslinked the two cysteine residues using bis-maleimidoethane (BMOE) to create XLcMT (Fig. 7). The BMOE crosslinker has an 8 \AA linker, which we hypothesized would fix the two termini at approximately the same distance apart as if the MT was embedded in the A domain. Both cMT and XLcMT were assayed for methyltransferase activity in the presence of either L-Phe-SNAC or L-Leu-SNAC. Crosslinking the N- and C-termini decreased the preference of the methyltransferase for L-Phe over L-Leu (Fig. 5). These data suggest that structural flexibility of the N- and/or C-terminus of MT_{BSLs} plays a role (either by allowing for a different stable conformation of the termini compared to the embedded MT or by providing flexibility at the termini) in the ability of the isolated MT to preferentially methylate L-Phe over L-Leu.

Although XLcMT $_{BSLs}$ displayed less preference for L-Phe-SNAC than MT_{BSLs} , the ratio of Phe:Leu methylated is still higher than that observed for the embedded MT. This could arise from a less than optimal cross-linking distance and incomplete desired

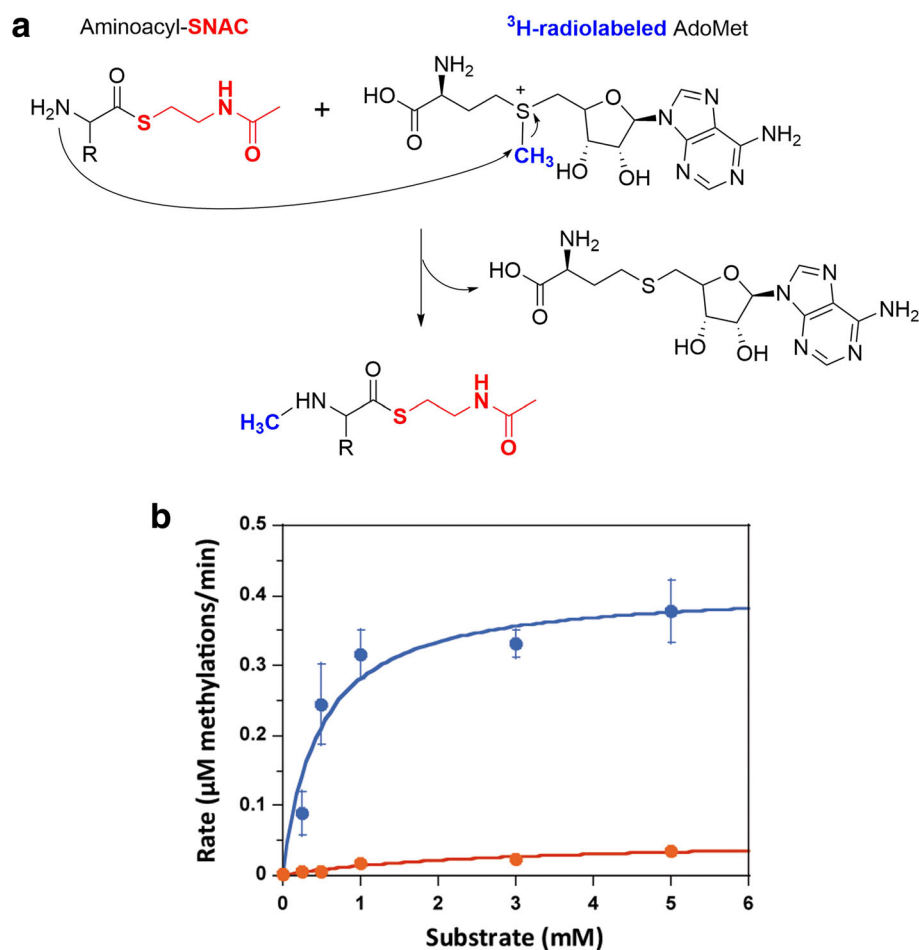


Fig. 4 In vitro methylation activity and substrate specificity of MT_{BSLs} . **a** Methylation was tracked using a 3H -labeled methyl group (highlighted in blue) from the co-substrate AdoMet. "R" represents amino acid side chain. **b** Concentration-dependent methylation rate of L-Phe-SNAC (blue trace) and L-Leu-SNAC (orange trace) by isolated MT_{BSLs}

crosslinking (~85–90%, Fig. 7). We therefore explored how adding a portion of the A domain might influence the ability of the isolated MT domain to differentially methylate L-Phe-SNAC. A construct containing just the small portion of the A domain was designed and purified (aMT_{BSLs}) (Figs. 5a and Additional file 1: Figure S8). When assayed in the presence of either L-Phe-SNAC or L-Leu-SNAC, the aMT_{BSLs} construct displayed little preference for L-Phe-SNAC, demonstrating levels of methylation that were similar to the full length BSLs (Fig. 5).

Discussion

NRPs represent a large family of structurally and functionally diverse natural products. Some of these molecules have shown health-benefiting biological activities and are used as pharmaceuticals, such as the well-known antibiotics penicillin and vancomycin. NRPs are synthesized by modular NRPSs which consist of a series of

catalytic domains. The domain structure and specificity of individual domains contribute to the chemical diversity in NRPs. Many different NRPSs, from bacteria or fungi, have been extensively investigated to understand the biosynthetic mechanisms. Based on the mechanistic studies, the enzymes can be engineered to create novel products through genetic approaches, such as domain swapping and active site modification [21]. Some reported NRPSs were found to contain a MT domain that is embedded in an A domain. In this work, we investigated BSLs, an iterative fungal NRPS to understand how embedding of the MT domain in an A domain affects the biosynthetic process and how the substrate specificity of MT is influenced by this unique structural feature.

To probe the role of the MT domain of BSLs in bassianolide biosynthesis, we removed this domain from BSLs. The resulting enzyme BSLs- Δ MT only yielded the non-methylated product *N*-desmethylbassianolide (Fig. 2a).

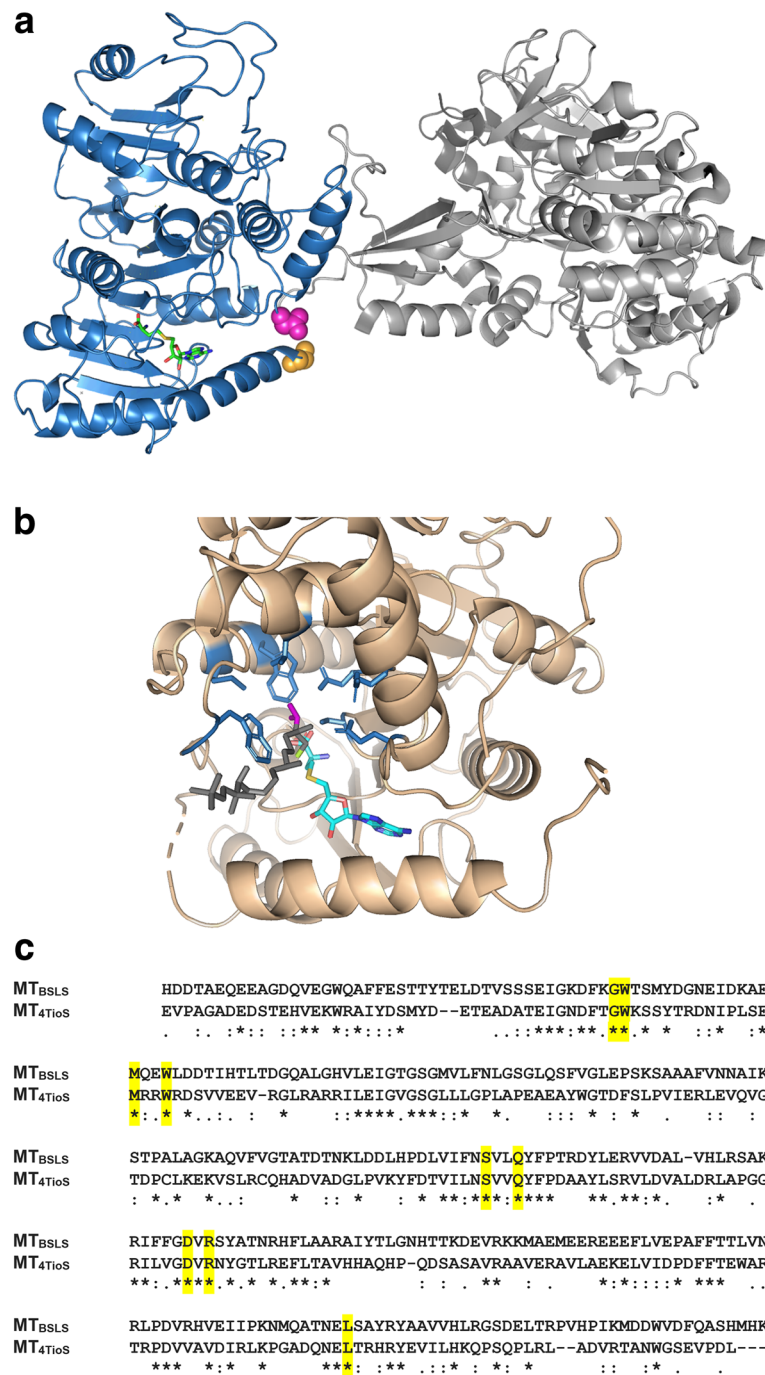
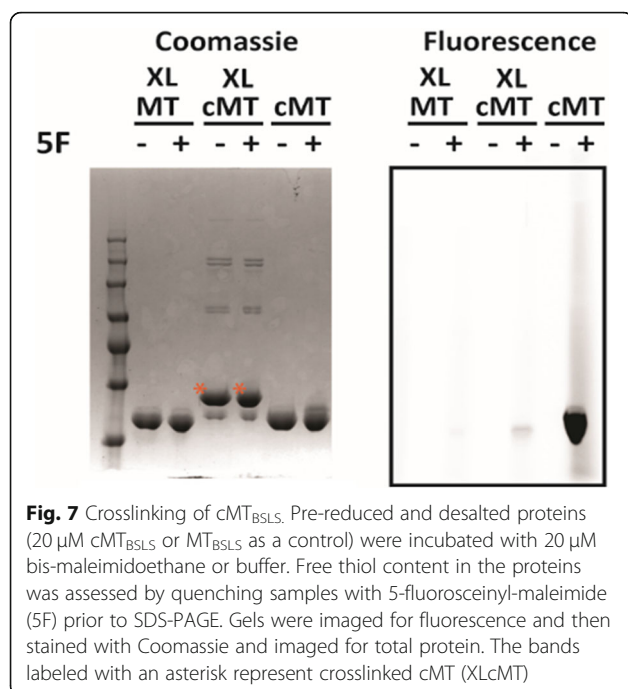


Fig. 6 Comparison of the MT domains of TioS and modeled BSLs. **a** A homology model for MT_{BSLS} generated with the Swiss-Model server using the MT-A structure from TioS(A_{4a}M₄A_{4b}) (pdb ID 5wmm). Sequence identity between the core of MT_{4TioS} and MT_{BSLS} is 32%. For context purposes, the A domain of TioS is shown in light gray. The generated model of MT_{BSLS} is shown in blue. The active site was identified by aligning the TioS structure (which contained S-adenosylhomocysteine, shown in green) with the MT_{BSLS} model. The N- and C-termini of MT_{BSLS} are shown in orange and magenta spheres, respectively. **b** The active site residues of the MT domain in TioS(A_{4a}M₄A_{4b}) (pdb ID 5wmm) that are proposed to interact with the valine side chain (magenta) of the enzyme-bound substrate (G525, W526, M540, W543, S632, Q635, D664, R666, and L738, shown in blue). The N-methylated product of the reaction (methyl group in green) was modeled into the active site [4]. **c** Residues in TioS(A_{4a}M₄A_{4b}) that interact with the substrate amino acid are conserved (yellow) in MT_{BSLS}



corresponding *N*-methylated products. Aminoacyl-SNACs were used to mimic the natural T-tethered substrates. A series of MT constructs, including BSLs, MT_{BSLS}, cMT, XLcMT, and aMT, were tested to compare the substrate specificity. The results show that the substrate specificity of MT_{BSLS} is modified by insertion into the A2 domain of BSLs. Among the five constructs, MT_{BSLS} showed a much higher methylation rate with L-Phe-SNAC than with L-Leu-SNAC. cMT showed a lower ratio of methylation of L-Phe-SNAC/L-Leu-SNAC, followed by XLcMT. This suggests that restricting both termini of the isolated MT increases the preference of this domain toward L-Leu-SNAC. aMT possessed a substrate specificity similar to the megaenzyme BSLs, likely due to its structural similarity to the megaenzyme (Additional file 1: Figure S8), further supporting that natural embedding of MT in the A2 domain is critical to narrow down the substrate specificity of the MT domain. Our data suggest that altered substrate specificity is mechanistically achieved by fixing the N- and/or C-terminus of the MT_{BSLS}. The somewhat relaxed substrate specificity of the isolated MT_{BSLS} suggests that this MT may be engineered to provide methylation of a variety of amino acids in designer NRPS systems. Embedding the MT could be used to afford selective methylation to the desired amino acid.

Our results also suggest a rationale for why the MT domain in this NRPS is embedded in the A domain instead of positioned as an end-on-end modifying unit or as a separate polypeptide. BSLs synthesizes both

bassianolide (Leu-containing) and beauvericins (Phe-containing) in ~ 5:1 ratio when expressed recombinantly in yeast [15]. This indicates that the A domain of BSLs is promiscuous and can activate both L-Leu and L-Phe. However, the MT domain showed a preference for L-Phe-SNAC over L-Leu-SNAC (Fig. 5B) and thus appears to be more promiscuous than the A domain. Embedding the MT tunes the activity of the MT domain against L-Phe, perhaps acting as a secondary gatekeeper. In naturally occurring NRPS systems, it may suggest that MT genes could be swapped/usurped from non-optimal NRPS clusters. Additionally, although the methyl group is not a necessary recognition element for the synthesis of bassianolide/beauvericin (deletion of the MT domain gave rise to a desmethyl product), the fact that we saw no evidence of transmethylation suggests that embedding the MT helps to ensure capture and methylation of the amino acid en route to formation of the NRP product.

Conclusions

In conclusion, we investigated the role of the MT domain in NRP biosynthesis and how its substrate specificity is affected by protein insertion. The MT domain of BSLs methylates the T-tethered amino acid precursors selected and activated by the A domain. The embedding of a functional MT domain in the A domain is not required for the biosynthesis of the NRP products, but is very critical for the overall efficiency of the assembly line. The substrate specificity of MT is significantly affected by the protein context within which it is present. While A domains are known to be responsible for selecting and activating the biosynthetic precursors for NRPS systems, our results suggest that embedding the MT acts as a secondary gatekeeper for the assembly line. This work thus provides new insights into the embedded MT domain in NRPSs, which will facilitate further engineering of this type of biosynthetic machinery to create structural diversity in natural products.

Methods

General methods and materials

Products were analyzed on an Agilent 1200 high performance liquid chromatography (HPLC) instrument. Mass spectra of the compounds were collected by the HPLC coupled with an Agilent 6130 Single Quad mass spectrometer. ¹H NMR data spectra were acquired on a JEOL instrument (300 MHz). High fidelity DNA polymerase, T4 DNA ligase, restriction enzymes and protein ladder were purchased from New England Biolabs. Other chemicals were purchased from Fisher Scientific. *B. bassiana* ATCC 7159 was obtained from American Type Culture Collection (ATCC). *S. cerevisiae* BJ5464-NpgA (*MAT ura3-52 his3-200 leu2-1 trp1 pep4::HIS3*

prb1 1.6R can1 GAL) was used as a host for heterologous expression, which was a gift from Dr. Nancy Da Silva at the University of California, Irvine. *E. coli* XL1-Blue and RIL were purchased from Stratagene for routine cloning and protein expression, respectively.

Synthesis of NAC

2.28 g cysteamine hydrochloride (20.0 mmol, 1.0 eq.), 1.12 g KOH (20.0 mmol, 1.0 eq.) and 5.04 g NaHCO₃ (60.0 mmol, 3.0 eq.) were dissolved in 100 mL of water. To the solution was dropwise added 1.9 mL of acetic anhydride (20.0 mmol, 1.0 eq.). The mixture was stirred at room temperature for 10 min. After adjusting the pH value to 7.3 by concentrated HCl, the resulting mixture was extracted with ethyl acetate (100 mL × 3). The combined organic extract was dried by anhydrous MgSO₄, filtered and concentrated in vacuo to give *N*-acetylcysteamine (NAC). ¹H NMR (300 MHz, CDCl₃): δ 5.92 (1H, br s), 3.42 (2H, q, *J* = 8.2 Hz), 2.67 (2H, m), 1.97 (3H, s), 1.35 (1H, t, *J* = 8.2 Hz).

Synthesis of aminoacyl-SNACs

Each tert-butyloxycarbonyl (Boc)-L-amino acid (1 mmol, 1.0 eq.), *N,N'*-dicyclohexylcarbodiimide (1 mmol, 1.0 eq.) and hydroxybenzotriazole (1 mmol, 1.0 eq.) were dissolved in 15 mL of trifluoroacetic acid (TFA), followed by adding 106 μL of NAC (1 mmol, 1.0 eq.). After stirring the resulting solution for 45 min at room temperature, 69.1 mg K₂CO₃ (0.5 mmol, 0.5 eq.) was added and the reaction mixture stirred for 3 h at room temperature. After filtered, the solvent was removed in vacuo. The residue dissolved in ethyl acetate and washed once with one volume of 10% aqueous NaHCO₃. The organic layer was dried by anhydrous MgSO₄, filtered and concentrated in vacuo. The crude product was subjected to silica gel column chromatography, eluted with 4% (v/v) MeOH-CHCl₃, to afford Boc-aminoacyl-SNACs. The Boc group was removed by dissolving the Boc-aminoacyl-SNAC in 50% TFA/CH₂Cl₂ and stirring at room temperature for 1 h. After evaporation of the solvents, the residue was taken up in a minimal volume of CH₂Cl₂ and precipitated with ether. The resulting solid was washed twice with ether and dried to afford the aminoacyl-SNACs. These synthetic SNAC derivatives were dissolved in deuterated dimethyl sulfoxide (DMSO-*d*₆) and their ¹H NMR spectra were collected. The chemical shift (δ) values are given in parts per million (ppm). The coupling constants (*J* values) are presented in hertz (Hz).

Boc-L-Leu-SNAC: ¹H NMR (300 MHz, DMSO-*d*₆): δ 7.97 (1H, br t, *J* = 5.5 Hz), 7.55 (1H, d, *J* = 7.9 Hz), 4.01 (1H, m), 3.10 (2H, m), 2.83 (2H, m), 1.75 (3H, s), 1.69 (1H, m), 1.59 (1H, m), 1.44 (1H, m), 1.37 (9H, s), 0.83 (3H, d, *J* = 6.5 Hz), 0.79 (3H, d, *J* = 6.5 Hz).

L-Leu-SNAC: ¹H NMR (300 MHz, DMSO-*d*₆): δ 8.58 (2H, br s), 8.11 (1H, br t, *J* = 5.5 Hz), 4.11 (1H, t, *J* = 6.9 Hz), 3.20 (2H, q, *J* = 6.5 Hz), 3.02 (2H, m), 1.77 (3H, s), 1.75 (1H, m), 1.61 (2H, t, *J* = 7.0 Hz), 0.88 (6H, d, *J* = 6.5 Hz); ESI-MS: [M + H]⁺ *m/z* 233.1.

Boc-L-Ile-SNAC: ¹H NMR (300 MHz, DMSO-*d*₆): δ 7.98 (1H, m), 7.50 (1H, d, *J* = 8.3 Hz), 3.90 (1H, dd, *J* = 7.9, 6.8 Hz), 3.12 (2H, m), 2.83 (2H, m), 1.75 (3H, s), 1.71 (1H, m), 1.52 (1H, m), 1.37 (9H, s), 1.18 (1H, m), 0.80 (3H, d, *J* = 6.8 Hz), 0.77 (3H, t, *J* = 7.0 Hz).

L-Ile-SNAC: ¹H NMR (300 MHz, DMSO-*d*₆): δ 8.42 (2H, br s), 8.06 (1H, br t, *J* = 5.5 Hz), 4.16 (1H, d, *J* = 4.1 Hz), 3.20 (2H, m), 3.02 (2H, m), 1.87 (1H, m), 1.76 (3H, s), 1.43 (1H, m), 1.22 (1H, m), 0.91 (3H, d, *J* = 6.9 Hz), 0.86 (3H, t, *J* = 7.4 Hz); ESI-MS: [M + H]⁺ *m/z* 233.1.

Boc-L-Val-SNAC: ¹H NMR (300 MHz, DMSO-*d*₆): δ 7.98 (1H, m), 7.49 (1H, d, *J* = 8.2 Hz), 3.87 (1H, dd, *J* = 8.3, 6.5 Hz), 3.12 (2H, m), 2.83 (2H, m), 2.04 (1H, m), 1.75 (3H, s), 1.38 (9H, s), 0.83 (6H, d, *J* = 6.9 Hz).

L-Val-SNAC: ¹H NMR (300 MHz, DMSO-*d*₆): δ 8.43 (2H, br s), 8.07 (1H, br t, *J* = 5.1 Hz), 4.12 (1H, d, *J* = 4.8 Hz), 3.20 (2H, m), 3.02 (2H, m), 2.16 (1H, m), 1.76 (3H, s), 0.96 (3H, d, *J* = 6.9 Hz), 0.92 (3H, d, *J* = 7.2 Hz). ESI-MS: [M + H]⁺ *m/z* 219.1.

Boc-L-Phe-SNAC: ¹H NMR (300 MHz, DMSO-*d*₆): δ 8.02 (1H, m), 7.62 (1H, d, *J* = 8.2 Hz), 7.22 (5H, m), 4.21 (1H, m), 3.13 (2H, m), 3.03 (1H, dd, *J* = 14.2, 4.3 Hz), 2.84 (2H, m), 2.76 (1H, dd, *J* = 14.2, 10.6 Hz), 1.76 (3H, s), 1.29 (9H, s).

L-Phe-SNAC: ¹H NMR (300 MHz, DMSO-*d*₆): δ 8.52 (2H, m), 8.01 (1H, t, *J* = 5.2 Hz), 7.25 (5H, m), 4.47 (1H, t, *J* = 6.9 Hz), 3.10 (4H, m), 2.95 (2H, m), 1.77 (3H, s). ESI-MS: [M + H]⁺ *m/z* 267.2.

Construction of expression plasmids

The cloning vector pJET1.2 (ThermoFisher Scientific) was used for general cloning. pET28a (Novagen) was used for protein expression in *E. coli*. The *E. coli*/*S. cerevisiae* shuttle vectors YEpADH2p-URA3 and YEpADH2p-TRP1 were used for expression or co-expression experiments in *S. cerevisiae* BJ5464-NpgA.

To construct BSLS-ΔMT in a yeast expression vector, we used pDY42 [12] as the starting plasmid. Our cloning strategy was to work on the fragment from the Bsu361 site (5518) to the C-terminal end (9441). Two pairs of primers, BSLS-Bsu3615518-F/BSLS-without-MT-R and BSLS-without-MT-F/2nd-BSLS-B-R-PmlI (Table 1), were used to perform SOE PCR to amplify a fragment without the MT domain, which was ligated to pJET1.2 to yield pDY254 (Table 2). After the plasmid was verified by sequencing, this fragment was excised by Bsu361 and PmlI and used to replace the original fragment from the 5518 to the end of *bsls* in pDY42 between the same sites, yielding pDY265 (Table 2).

Table 1 Primers used in this study

Primer	Sequence	Restriction sites
BEAS-S2131A-F	5'-CCTGGAGATTGGAACCGCTACAGGTATGATCTTGTT-3'	None
BEAS-S2131A-R	5'-ACATGCCCGGTACATGACCGTCGCGTAGAGTAT-3'	None
BSLS-Bsu3615518-F	5'-AACCTCAGGATGCTGTCGATGCG-3'	Bsu361
BSLS-without-MT-R	5'-CACCGCCACACGTCGCTTTCCGCAACCACAAATCCG-3'	None
BSLS-without-MT-F	5'-CGGATTTGTGGTTGCGGAAAAGCGACGTGTGGCGGTG-3'	None
2nd-BSLS-B-R-PmlI	5'-AACACGTGTAAGACGCATTCAAAGCCT-3'	PmlI
MT _{BSLS} -F-NheI	5'-AAGCTAGCCACGACGACACTGCCGAACA-3'	NheI
MT _{BSLS} -R-EcoRI	5'-AAGAATTCTCACTGAAGTCGCTGGAGAGGTT-3'	EcoRI
MT _{BSLS} -F-NdeI	5'-AACATATGCACGACGACACTGCCGAACA-3'	NdeI
MT _{BSLS} -R-PmeI	5'-AAGTTTAAACTCACTGAAGTCGCTGGAGAGGTT-3'	PmeI
MT _{BEAS} -F-NdeI	5'-AACATATGGCTGACGATGCCGTTGAGCA-3'	NdeI
MT _{BEAS} -R-PmeI	5'-AAGTTTAAACCTGCAGCCGCTGCAGCGGCC-3'	PmeI
aMT _{BSLS} -F-SpeI	5'-AAACTAGTCAATTCAAGATTCGAAGTAACCGCATC-3'	SpeI
aMT _{BSLS} -R-EcoRI	5'-AAAGAATTCTCACGCCACAATGTGGGAAG-3'	EcoRI
cMT _{BSLS} -F-NheI	5'-AAAGCTAGCTGCGTTGCGGAACACG-3'	NheI
cMT _{BSLS} -R-EcoRI	5'-TTTGAATTCTCAGCACTGGAGAGGTTGATTGGTGAG-3'	EcoRI

The YEpADH2p-URA3 derived *beas*-harboring plasmid pDY37 [12] was used as the template for PCR with a pair of primers, BEAS-S2131A-F and BEAS-S2131A-R (Table 1). The mutated nucleotide was included in BEAS-S2131A-F. The PCR product was treated with DpnI at 37 °C for 24 h to digest the template. T4 DNA ligase was then added to ligate the PCR product, which was then introduced into *E. coli* XL-Blue through chemical transformation. Correct clones were selected by ampicillin resistance and confirmed by digestion check and sequencing. The correct BEAS-G2131A plasmid was named pDY170 (Table 2).

The gene encoding the MT domain of BSLS was amplified via PCR from the genomic DNA of *B. bassiana* using primers MT_{BSLS}-F-NheI and MT_{BSLS}-R-EcoRI (Table 1). The PCR product was ligated into pJET1.2 and introduced into *E. coli* XL1-Blue to afford pZJ135 (Table 2). pZJ135 was digested with NheI and EcoRI, and the fragment was ligated into pET28a between the corresponding restriction sites to yield pJCZ22 (Table 2). The same MT domain was amplified with MT_{BSLS}-F-NdeI and MT_{BSLS}-R-PmeI and ligated into pJET1.2 to yield pFC30 (Table 2). The gene fragment was then excised using NdeI and PmeI

Table 2 Plasmids used in this study

Plasmid	Description	Restriction sites	Source
pDY37	<i>beas</i> in YEpADH2p-URA3	NheI and PmlI	[12]
pDY42	<i>bsls</i> in YEpADH2p-URA3	NdeI and PmlI	[12]
pDY170	<i>beas</i> -G2131A in YEpADH2p-URA3	NheI and PmlI	This work
pDY254	<i>bsls</i> ₍₅₈₁₈₋₉₄₃₈₎ - Δ mt in pJET1.2	Bsu361 and PmlI	This work
pDY265	<i>bsls</i> - Δ mt in YEpADH2p-URA3	Bsu361 and PmlI	This work
pDY267	MT _{BEAS} in pJET1.2	NdeI and PmeI	This work
pDY268	MT _{BEAS} in YEpADH2p-TRP1	NdeI and PmeI	This work
pFC30	MT _{BSLS} in pJET1.2	NdeI and PmeI	This work
pFC31	MT _{BSLS} in YEpADH2p-TRP1	NdeI and PmeI	This work
pZJ135	MT _{BSLS} in pJET1.2	NheI and EcoRI	This work
pJCZ22	MT _{BSLS} in pET28a	NheI and EcoRI	This work
paMTBSLS	aMT _{BSLS} in pET28a (a small portion of the A ₂ domain+MT of BSLS)	NheI and EcoRI	This work
pcMTBSLS	cMT _{BSLS} in pET28a (MT of BSLS containing an additional cysteine residue at both the N- and C-termini of the MT domain)	NheI and EcoRI	This work

and ligated into YEpADH2p-TRP1 between the same sites to yield pFC31 (Table 2). Similarly, the MT domain of BEAS was amplified with MT_{BEAS}-F-NdeI and MT_{BEAS}-R-PmeI and ligated into pJET1.2 to afford pDY267 (Table 2). The MT_{BEAS} gene fragment was excised from pDY267 using NdeI and PmeI and ligated into YEpADH2p-TRP1 between the same sites to yield pDY268 (Table 2).

The gene for the aMT_{BLSL} construct, which also contains the small fragment of the A2 domain, was amplified using primers aMT_{BLSL}-F-SpeI and aMT_{BLSL}-R-EcoRI (Table 1). The digested PCR product was ligated into NheI/EcoRI digested pET28a to yield paMTBLSL (Table 2). The gene for the cMT_{BLSL} construct, which contains an additional cysteine residue at both the N- and C-termini, was amplified using primers cMT_{BLSL}-F-NheI and cMT_{BLSL}-R-EcoRI. The digested PCR product was ligated into pET28a between the NheI and EcoRI sites to yield pcMTBLSL (Table 2). All plasmids were verified by DNA sequencing.

Expression and purification of MT constructs

The 348 kDa BLSL was expressed in *S. cerevisiae* BJ5464-NpgA/pDY42 (Table 2) and purified using Ni-NTA chromatography as described in our previous work [11]. To purify MT_{BLSL}, pJCZ22 was introduced into *E. coli* RIL. The resulting strain was grown at 37 °C in Luria-Bertani (LB) medium supplemented with 35 µg mL⁻¹ kanamycin and 25 µg mL⁻¹ chloramphenicol to an OD₆₀₀ of 0.4–0.6, and induced by 200 µM isopropyl-1-thio-β-D-galactoside (IPTG) for 16 h at 28 °C. The cells were harvested by centrifugation at 3,500 rpm for 10 min, re-suspended in 30 mL of cold lysis buffer [20 mM Tris-HCl (pH 7.9), 0.5 M NaCl, pH 7.9] and sonicated on ice. Cellular debris was removed by centrifugation at 20,000 rpm for 30 min at 4 °C. Ni-NTA agarose resin (Qia-gen) was added to the supernatant (4 mL L⁻¹ of culture) and the mixture was shaken at 4 °C for 4 h to ensure the His₆-tagged protein was well absorbed. The protein resin mixture was loaded into a gravity flow column and protein was purified with an increasing concentration of imidazole in buffer A [50 mM Tris-HCl, pH 7.9, 2 mM ethylenediaminetetraacetic acid (EDTA), 1 mM dithiothreitol (DTT) and 0.2 mM phenylmethylsulfonyl fluoride (PMSF)]. The purified MT_{BLSL} was concentrated and washed with 50 mM Tris-HCl buffer (pH 7.9) by Centriprep filter devices (Amicon Inc.).

The cMT_{BLSL} and aMT_{BLSL} proteins were expressed in *E. coli* RIL cells with 200 µM IPTG for 24 h at 16 °C. Cells were resuspended in the lysis buffer, lysed by sonication, and centrifuged as noted above. Clarified lysate was incubated with Goldbio Nickel resin (0.5 mL resin/g of cells) for 4 h while shaking at 4 °C. The nickel resin was batch-washed and the desired proteins eluted with a

stepped imidazole gradient. An additional anion exchange step (MonoQ) was required to purify the aMT_{BLSL} construct. Protein purity was evaluated by sodium dodecyl sulfate polyacrylamide gel electrophoresis (SDS-PAGE). Selected fractions were pooled and concentrated in a 30 K MWCO Millipore spin concentrator that was also used to exchange the buffer (50 mM Tris-HCl, 150 mM NaCl, 2 mM β-mercaptoethanol, 5% glycerol, pH 7.5). Proteins were frozen in liquid nitrogen and stored at – 80 °C.

Production of *N*-desmethylated NRPs using engineered yeast strains

pDY265 and pDY170 were respectively transferred into *S. cerevisiae* BJ5464-NpgA. The strains were grown in SC-URA medium as described in our previous work [12]. The products were extracted with ethyl acetate and analyzed by LC-MS using a Zorbax SB-C18 reversed-phase column (5 µm, 150 mm × 4.6 mm) at 210 nm, washed with a gradient of methanol-water (80 to 100% over 20 min) at a flow rate of 1 mL min⁻¹. The demethylated derivative of beauvericin was isolated by HPLC from 1 L of culture of *S. cerevisiae* BJ5464-NpgA/pDY170 for NMR analysis (Additional file 1: Figures S2–S4).

For co-expression of an isolated MT domain with BLSL-ΔMT or BEAS-G2121A, pFC31 and pDY265, or pDY268 and pDY170, were co-transferred into *S. cerevisiae* BJ5464-NpgA. The strains were grown in SC-URA-TRP medium, and the products were extracted and analyzed as described above.

LC-MS identification of methylated products of aminoacyl SNACs

A typical methylation assay mixture (100 µL) consisted of 6.4 µM MT_{BLSL}, 0.8 mM aminoacyl-SNAC, and 2.4 mM AdoMet in 100 mM Tris-HCl buffer (pH 7.5). The reaction mixtures were incubated at 25 °C for 30 min and then quenched with MeOH (50 µL). Substrate controls included all the components except MT_{BLSL}. The mixtures were briefly vortexed and centrifuged at 15,000 rpm for 5 min to remove the precipitated protein before the samples were injected into LC-MS for analysis. The supernatants were analyzed on an Agilent Single Quad LC-MS by using a Zorbax SB-C18 reversed-phase column (5 µm, 150 mm × 4.6 mm) at 235 nm, eluted with a solvent gradient of increasing acetonitrile (10–15%) in H₂O containing 0.1% trifluoroacetic acid with a flow rate of 1 mL min⁻¹.

Quantification of the activity of the MT domains

Methyltransferase activity was quantified using a radiometric approach. Methylation reactions were conducted in 50 mM Na₂HPO₄, [pH 7.5], 100 µM AdoMet (99 µM

unlabeled AdoMet and 1 μM *S*-[methyl- ^3H]-AdoMet (PerkinElmer Life Sciences; stock solution of 5–10 mM (~ 75 Ci/mmol) in 10 mM $\text{H}_2\text{SO}_4/\text{EtOH}$ (9,1, v/v)) and 1.5 μM enzyme in a total volume of 25 μL . The reactions were initiated with amino acyl-SNAC substrates at varying concentrations as indicated in the figures and incubated at 25 $^\circ\text{C}$. Aliquots (10 μL) at various times were removed from the reaction and placed in 20 μL of 1 M Tris-HCl buffer (pH 9.8) and immediately diluted by the addition of 200 μL of H_2O . The *N*-methylated product was extracted using 400 μL of ethyl acetate. Half the organic layer was added to 4.8 mL of scintillation cocktail and the radioactivity present quantified using scintillation counting.

Crosslinking of methyltransferases

Proteins undergoing crosslinking were first pre-reduced with 1 mM DTT for 20 min and rapidly desalted using Zebaspin columns (Pierce). Crosslinking was accomplished by incubating 20 μM protein (cMT_{BLSL}, or MT_{BLSL} as a control) with 20 μM bis-maleimidoethane (BMOE) on ice for 1 h. For gel analyses, samples were either treated with 5-fluorosceinyl-maleimide (5F) in SDS sample buffer lacking β -mercaptoethanol for 10 min, followed by a DTT quench step, or were treated with SDS sample buffer containing β -mercaptoethanol for 10 min, followed by a DTT quench step. SDS-gels were first imaged for fluorescence resulting from the covalent addition of 5F to free thiols and then stained with Coomassie. The per cent of desired crosslinking (noted by the asterisk in Fig. 7) was estimated at 85–90% by taking the intensity of the desired band (measured by densitometry) divided by the total intensity of all bands in the lane. For crosslinking prior to activity measurements, cMT_{BLSL} was pre-reduced and incubated in the presence and absence (control) of the BMOE crosslinker as described above. After 1 h the reactions were quenched with 2 mM DTT and desalted using Zebaspin columns.

Additional file

Additional file 1: Figure S1. ESI-MS (+) spectra of the demethylated nonribosomal peptides. (A) *N*-Desmethylbassianolide. (B) *N*-Desmethylbeauvericin. (C) *N*-Desmethylbeauvericin A. (D) *N*-Desmethylbeauvericin B. **Figure S2.** ^1H NMR spectrum of *N*-desmethylbeauvericin. **Figure S3.** ^{13}C NMR spectrum of *N*-desmethylbeauvericin. **Figure S4.** Selected ^1H - ^1H COSY and HMBC correlations for *N*-desmethylbeauvericin. **Figure S5.** HPLC analysis (210 nm) of products from the co-expression of isolated MT domain with MT-removed BSL/MT-inactivated BEAS in *S. cerevisiae*. (A) Co-expression of MT_(BSL) with BSL- Δ MT. (B) Co-expression of MT_(BEAS) with BEAS-G2131A. **Figure S6.** ESI-MS(+) spectrum of the *N*-methylated products of L-Ile-SNAC (A) and L-Val-SNAC. **Figure S7.** Location of residues in MT_{BLSL} that are proposed to interact with the amino acid substrate. The active site residues (red) of the MT domain in TioS(A_{4a}M₄A_{4b}) (pdb ID 5wmm) (gray) that are proposed to interact with the valine side chain (magenta) of the enzyme-bound substrate (G525, W526, M540, W543, S632, Q635, D664,

R666, and L738) were mapped onto the homology model of MT_{BLSL} (blue, with limon amino acid side chains). AdoHcy is shown in green and the tethered substrate for TioS(A_{4a}M₄A_{4b}) is shown in dark gray. **Figure S8.** Architecture of the aMT construct. Adenylation domains consist of one polypeptide containing a large subunit (light gray) and a small subunit (dark gray). The active site exists between the two subunits. The "aMT" construct used in these studies contains the entire MT domain and the small subunit of the adenylation domain. Figure 6a was used in the preparation of this figure. (DOCX 1951 kb)

Abbreviations

5F: 5-Fluorosceinyl-maleimide; A: Adenylation; AdoMet: *S*-Adenosyl methionine; Aminoacyl-SNACs: Aminoacyl-*N*-acetylcysteamine thioesters; BEAS: Beauvericin synthetase; BMOE: Bis-Maleimidoethane; Boc: Tert-Butyloxycarbonyl; BSL: Bassianolide synthetase; C: Condensation; D-Hiv: D-2-Hydroxyisovalerate; D-Hmv: D-2-Hydroxy-3-methylvalerate; DTT: Dithiothreitol; E: Epimerization; EDTA: Ethylenediaminetetraacetic acid; HPLC: High performance liquid chromatography; IPTG: Isopropyl-1-thio- β -D-galactoside; MS: Mass spectrometry; MT: Methyltransferase; NAC: *N*-Acetylcysteamine; NCA: Norcoronamic acid; NRP: Nonribosomal peptide; NRPS: Nonribosomal peptide synthetase; PKS: Polyketide synthase; PMSF: Phenylmethylsulfonyl fluoride; SDS-PAGE: Sodium dodecyl sulfate polyacrylamide gel electrophoresis; T: Thiolation; TE: Thioesterase; TFA: Trifluoroacetic acid

Acknowledgments

The authors wish to thank Miekian Stonhill for her technical expertise in cloning, expression, and purification of some of the MT constructs. The authors also thank Oleg Tsodikova and Sylvie Garneau-Tsodikova for providing the structural model of TioS(A_{4a}M₄A_{4b}) bound with *S*-adenosyl homocysteine and PPant-*N*-methyl-L-Val shown in Fig. 5b.

Authors' contributions

JH and JZhan conceived of and supervised this study. FX, DY, JZi and JZeng conducted the gene cloning work and constructed the expression plasmids for *S. cerevisiae* and *E. coli*. FX conducted the yeast expression work and in vitro reactions of MT_{BLSL} with aminoacyl-SNACs. RB, KM and MR constructed paMT_{BLSL} and pcMT_{BLSL}, purified the MT constructs, performed the kinetic studies, and measured the activity of the MT domain and its variants. All the authors analyzed the data and contributed to the writing of this manuscript. All authors read and approved the final manuscript.

Funding

This work was supported by a Utah State University Research Catalyst grant (JZhan and JH) and grants from the National Natural Science Foundation of China (31170763, 31470787, DY).

Availability of data and materials

Data and materials are available from the corresponding authors upon reasonable request.

Ethics approval and consent to participate

Not applicable.

Consent for publication

Not applicable.

Competing interests

The authors declare that they have no competing interests.

Author details

¹Department of Biological Engineering, Utah State University, 4105 Old Main Hill, Logan, UT 84322-4105, USA. ²Department of Chemistry and Biochemistry, Utah State University, 0300 Old Main Hill, Logan, UT 84322-0300, USA. ³Department of Applied Chemistry and Biological Engineering, College of Chemical Engineering, Northeast Electric Power University, Jilin 132012, Jilin, China. ⁴Key Laboratory of Modern Preparation of TCM, Ministry of Education, Jiangxi University of Traditional Chinese Medicine, Nanchang 330004, Jiangxi, China.

Received: 1 June 2019 Accepted: 17 July 2019

Published online: 31 July 2019

References

- Fischbach MA, Walsh CT. Assembly-line enzymology for polyketide and nonribosomal peptide antibiotics: logic, machinery, and mechanisms. *Chem Rev.* 2006;106(8):3468–96.
- Süssmuth RD, Mainz A. Nonribosomal peptide synthesis—principles and prospects. *Angew Chem Int Ed.* 2017;56(14):3770–821.
- Ansari MZ, Sharma J, Gokhale RS, Mohanty D. In silico analysis of methyltransferase domains involved in biosynthesis of secondary metabolites. *BMC Bioinformatics.* 2008;9:454.
- Mori S, Pang AH, Lundy TA, Garzan A, Tsodikov OV, Garneau-Tsodikova S. Structural basis for backbone N-methylation by an interrupted adenylation domain. *Nat Chem Biol.* 2018;14(5):428–30.
- Ostermeier M. Engineering allosteric protein switches by domain insertion. *Protein Eng Des.* 2005;18(8):359–64.
- Aroul-Selvam R, Hubbard T, Sasidharan R. Domain insertions in protein structures. *J Mol Biol.* 2004;338(4):633–41.
- Xu Y, Orozco R, Wijeratne EMK, Espinosa-Artiles P, Gunatilaka AAL, Stock SP, et al. Biosynthesis of the cyclooligomer depsipeptide bassianolide, an insecticidal virulence factor of *Beauveria bassiana*. *Fungal Genet Biol.* 2009;46(5):353–64.
- Xu Y, Orozco R, Wijeratne EMK, Gunatilaka AAL, Stock SP, Molnar I. Biosynthesis of the cyclooligomer depsipeptide beauvericin, a virulence factor of the entomopathogenic fungus *Beauveria bassiana*. *Chem Biol.* 2008;15(9):898–907.
- Zhan J, Burns AM, Liu MX, Faeth SH, Gunatilaka AAL. Search for cell motility and angiogenesis inhibitors with potential anticancer activity: Beauvericin and other constituents of two endophytic strains of *Fusarium oxysporum*. *J Nat Prod.* 2007;70(2):227–32.
- Jirakkakul J, Punya J, Pongpattanakitshote S, Paungmoung P, Vorapreeda N, Tachaleat A, et al. Identification of the nonribosomal peptide synthetase gene responsible for bassianolide synthesis in wood-decaying fungus *Xylaria* sp. BCC1067. *Microbiology.* 2008;154(4):995–1006.
- Yu D, Xu F, Zhang S, Zhan J. Decoding and reprogramming fungal iterative nonribosomal peptide synthetases. *Nat Commun.* 2017;8:15349.
- Yu D, Xu F, Zi J, Wang S, Gage D, Zeng J, et al. Engineered production of fungal anticancer cyclooligomer depsipeptides in *Saccharomyces cerevisiae*. *Metab Eng.* 2013;18:60–8.
- Kagan RM, Clarke S. Widespread occurrence of three sequence motifs in diverse S-adenosylmethionine-dependent methyltransferases suggests a common structure for these enzymes. *Arch Biochem Biophys.* 1994;310(2):417–27.
- Ehmann DE, Trauger JW, Stachelhaus T, Walsh CT. Aminoacyl-SNACs as small-molecule substrates for the condensation domains of nonribosomal peptide synthetases. *Chem Biol.* 2000;7(10):765–72.
- Yu D, Xu F, Gage D, Zhan J. Functional dissection and module swapping of fungal cyclooligomer depsipeptide synthetases. *Chem Commun.* 2013;49(55):6176–8.
- Waterhouse A, Bertoni M, Bienert S, Studer G, Tauriello G, Gumienny R, et al. SWISS-MODEL: homology modelling of protein structures and complexes. *Nucleic Acids Res.* 2018;46(W1):W296–303.
- Bienert S, Waterhouse A, de Beer TAP, Tauriello G, Studer G, Bordoli L, et al. The SWISS-MODEL repository—new features and functionality. *Nucleic Acids Res.* 2017;45(D1):D313–9.
- Guex N, Peitsch MC, Schwede T. Automated comparative protein structure modeling with SWISS-MODEL and Swiss-PdbViewer: a historical perspective. *Electrophoresis.* 2009;30(Suppl 1):S162–73.
- Benkert P, Biasini M, Schwede T. Toward the estimation of the absolute quality of individual protein structure models. *Bioinformatics.* 2011;27(3):343–50.
- Bertoni M, Kiefer F, Biasini M, Bordoli L, Schwede T. Modeling protein quaternary structure of homo- and hetero-oligomers beyond binary interactions by homology. *Sci Rep.* 2017;7(1):1–15.
- Winn M, Fyans JK, Zhuo Y, Micklefield J. Recent advances in engineering nonribosomal peptide assembly lines. *Nat Prod Rep.* 2016;33(2):317–47.
- Velkov T, Horne J, Scanlon MJ, BenCapuano YE, Lawen A. Characterization of the N-methyltransferase activities of the multifunctional polypeptide cyclosporin synthetase. *Chem Biol.* 2011;18(4):464–75.
- Xu Y, Zhou T, Zhou Z, Su S, Roberts SA, Montfort WR, et al. Rational reprogramming of fungal polyketide first-ring cyclization. *Proc Natl Acad Sci U S A.* 2013;110(14):5398–403.

Publisher's Note

Springer Nature remains neutral with regard to jurisdictional claims in published maps and institutional affiliations.

Ready to submit your research? Choose BMC and benefit from:

- fast, convenient online submission
- thorough peer review by experienced researchers in your field
- rapid publication on acceptance
- support for research data, including large and complex data types
- gold Open Access which fosters wider collaboration and increased citations
- maximum visibility for your research: over 100M website views per year

At BMC, research is always in progress.

Learn more biomedcentral.com/submissions

